Role of YWHAG in cell proliferation in gastric cancer

Yumin Li

liym@lzu.edu.cn

Lanzhou University Second Hospital https://orcid.org/0000-0002-9267-1412

Luxi Yang

Lanzhou University Second Hospital https://orcid.org/0000-0002-5242-7642

Yanmei Gu

Jicheng Li

Xiaomei Li

Songlin Songlin Wu

Article

Keywords: YWHAG, Gastric cancer, Proliferation, Migration, PI3K/AKT

Posted Date: December 28th, 2023

DOI: https://doi.org/10.21203/rs.3.rs-3667504/v1

Additional Declarations: There is **NO** conflict of interest to disclose.

Abstract

The role of tyrosine 3-monooxygenase/tryptophan 5-monooxygenase activation protein gamma (YWHAG) in gastric cancer (GC) remains unclear. In this study, we investigated its biological effects on GC as well as the associated molecular mechanisms. We evaluated YWHAG expression in GC and normal tissues, and using GC cells with YWHAG knockdown or overexpression, we examined GC cell viability and growth. We also performed experiments to determine GC cell cycle progression, apoptosis, migration, and invasion. We also verified the role of YWHAG in GC growth using a mouse xenograft tumor model and performed Gene Set Enrichment Analysis (GSEA) and western blot analysis to elucidate possible molecular mechanisms. Our results showed a significantly higher YWHAG expression level in GC tissues ($p < 0.0001$), especially in poorly differentiated GC tissues ($p < 0.0001$). Further, YWHAG knockdown significantly inhibited GC cell proliferation, migration, invasion, and epithelial-mesenchymal transformation; however, these effects were reversed via YWHAG overexpression. Furthermore, YWHAG downregulation significantly retarded the growth of xenograft tumors in mice, and mechanistically, YWHAG exerted oncogenic effects in GC by activating the PI3K/AKT pathway. Therefore, YWHAG promotes GC growth, functions as an oncogene, and has potential as a therapeutic target in GC.

Introduction

Gastric cancer (GC) is the fifth most common type of cancer and one of the leading cause of cancer-related deaths globally [1]. Recently, decreases in the incidence and mortality of GC have been reported; however, many patients still experience postoperative recurrence and chemotherapy resistance [2, 3]. Therefore, it is imperative to identify therapeutic targets that can be used to improve the survival of patients with GC.

The tyrosine 3-monooxygenase/tryptophan 5-monooxygenase activation protein (YWHA) 14-3-3 family regulates numerous cellular processes, including cell metabolism, signal transduction, and cell cycle apoptosis. It has also been shown that this family of proteins may cause conformational changes in their binding partners by binding to phosphoserine-containing proteins[4]. Specifically, YWHAG (14-3-3γ), a member of the YWHA protein family, was identified and isolated in 1999[5], and studies have indicated that it is overexpressed in malignances, such as glioblastoma and breast cancer [5–7]. It has also been shown to act as an oncogene in advanced lung cancer and it indirectly downregulate p53 [7]. Moreover, it inhibits apoptosis in breast cancer and facilitates metastasis [8, 9]. Mei et al. reported that miRNAs can promote epithelial-mesenchymal transformation (EMT) in breast cancer cells by targeting YWHAG [10]. In summary, YWHAG plays an important modulatory role in malignant tumors and may be an attractive molecular target for cancer treatment. However, its effects and regulatory mechanisms in GC remain unclear.

In this study, we aimed to investigate the biological effects of YWHAG on GC and clarify the related mechanisms. Thus, we investigated the expression pattern of YWAHG in GC tissues via immunohistochemistry (IHC), and thereafter, performed correlation analysis. GC cell lines with stable

YWHAG knockdown and overexpression were generated to evaluate the biological functions of YWHAG in vitro and in vivo. Thus, our results indicated that in GC tissues, YWHAG is positively associated with cell proliferation, apoptosis, cell cycle, migration, and invasion. Additionally, our results highlighted a potential mechanism in GC progression mediated by YWHAG, and suggest that YWHAG, which plays an essential role in GC, may be a potential therapeutic target in GC.

Materials and methods

Clinical specimens

A total of 107 pairs of GC and normal tissue samples were collected from May 2013 to December 2014 at the Lanzhou University Second Hospital, Gansu, China. The collection of the tissue samples was approved by the Ethics Committee of the abovementioned institution (approval no. 2021A-153). Further, all the patients provided informed consent before specimen collection and did not receive any treatment before surgery.

IHC

Paraffin-embedded tissue sections were dewaxed and hydrated, and after antigen retrieval, soaked in 0.3% H_2O_2 to block endogenous peroxidase activity. This was followed by incubation with anti-YWHAG (ab237732, 1:200; Abcam, Cambridge, MA, USA) and anti-Ki67 (ab15580, 1:300; Abcam) overnight at 4°C and staining with diaminobenzidine and counterstaining with hematoxylin. Next, IHC was independently performed by two senior pathologists blinded to the method. The scores for the tissues were determined based on the percentage of stained cells (0 = 0–5%, 1 = 6–25%, 2 = 26–50%, 3 = 51–75%, 4 = 76–100%) and the intensity of the staining (0 = no staining, 1 = weak staining, 2 = moderate staining, and 3 = strong staining). The product of these two scores yielded the final YWHAG and Ki67 scores.

Bioinformatics analysis

GC transcription data, corresponding to 375 samples, were obtained from The Cancer Genome Atlas (TCGA) database (https://ancergenome.nih.gov/), and YWHAG expression was analyzed using R software (R Development Core Team, Vienna, Austria). Further, the Gene Set Enrichment Analysis (GSEA) software was used to determine the potential roles of YWHAG in GC.

Cell culture

Human GC cell lines MKN45, HGC27, NCI-N87, MKN28, KAO-III, AGS, and normal human gastric mucosal epithelial cells (GES-1) were purchased from the Cell Culture Center of the Chinese Academy of Medical Sciences (Beijing, China). All cell lines were identified based on short tandem repeats (STR) and were maintained in RPMI 1640 medium (Gibco, Carlsbad, CA, USA) with 10% fetal bovine serum (FBS, Gibco) at 37 ℃ in a humidified incubator with 5% CO_2.

Lentivirus transfection

YWHAG overexpression and knockdown lentiviruses (GeneChem, Shanghai, China) were separately transfected into NCI-N87 and MKN45 cell lines. An empty lentiviral vector was used as the negative control. Seventy-two hours after transfection, the cells were selected using puromycin (Biofroxx, Berlin, Germany) for 3 days. Thereafter, transfection efficiency was verified via western blot analysis.

Cell counting kit-8 (CCK8) assay

GC cells were seeded in a 96-well plate and cultured in an incubator at 37°C. At the specific time points, 10 μl of the CCK8 assay solution (Beyotime Biotechnology, Shanghai, China) was added and followed by incubation for 1 h. Finally, absorbance measurements were performed at 490 nm.

EdU assay

Cells were seeded in 96-well plates at a density of 2×10^3 cells/well and incubated with EdU (RiboBio, Guangzhou, China) for 2 h. After fixing with 4% paraformaldehyde, the cells were stained according to the manufacturer's instructions. Finally, the Operetta CLS High Content Screening System (PerkinElmer, Waltham, MA, USA) was used to measure the percentage of EdU-positive cells.

Cell cycle and apoptosis detection

Cells were resuspended in 100 μl binding buffer, and the concentration was adjusted to 2×10^5 cells/tube. Thereafter, the cells were fixed overnight in 75% ethanol at 4°C. This was followed by staining with propidium iodide (PI; BD Bioscience, San Diego, CA, USA). Then, to examine apoptosis, the cells were stained with Annexin V-FITC/PI (BD Bioscience) and incubated in the dark at room temperature (22℃). Finally, flow cytometry was performed to determine apoptosis rate and cycle distribution.

Migration assay

The invasive ability of GC cells was evaluated via transwell coating with a matrix (BD Bioscience). Briefly, 5×10^4 cells were resuspended in serum-free medium and added to the upper chamber of a transwell assay kit. Next, medium containing 10% FBS was added to the lower chamber as a chemical attractant. Cells on the membrane surface were wiped clean using a cotton swab after 24 h. Then, the cells that migrated to the lower chamber were fixed with 4% paraformaldehyde and stained with 0.1% crystal violet. The number of invading cells was then counted using a microscope (OLYMPUS BX50, Japan).

Further, when the cells attained 90% confluence, a sterile 200 μl pipette tip was used to form a scratch wound on the cell monolayer. Next, the cells were washed twice with PBS and cultured in a serum-free medium. Wound width was then measured at 0, 24, 48, and 72 h.

Western blot analysis

GC cells were lysed on ice using a radioimmunoprecipitation assay (RIPA) buffer containing protease inhibitors. Equal amounts of protein were separated using 10%SDS-PAGE and transferred to a polyvinylidene fluoride (PVDF) membranes, which were then sealed with a blocking solution for 2 h. Next, the membranes were incubated with the corresponding primary antibodies overnight at 4 ℃. The

primary antibodies used included: anti-GAPDH (60004-1-Ig, 1:10000; Proteintech, Wuhan, China), anti-YWHAG (ab237732, 1:1000; Abcam), anti-cyclinD1 (60186-1-Ig, 1:5000; Proteintech), anti-CDK2 (10122-1-AP, 1:5000; Proteintech), anti-E-cadherin (20874-1-AP, 1;1000; Proteintech), anti-vimentin (10366-1-AP, 1:2000; Proteintech), anti-AKT (9272S, 1:1000; Cell Signaling Technology, Berkeley, CA. USA), anti-p-AKT (4060S, 1:2000; Cell Signaling Technology), and anti-p-PI3K (17366S, 1:1000; Cell Signaling Technology, USA). The cell membranes were then incubated with secondary antibodies and exposed to a chemiluminescence detection system.

Tumor xenograft model

Ten female BALB/c nude mice aged 5–6 weeks were purchased from Ziyuan Laboratory Animal Technology Co., Ltd. (Hangzhou, China). All the mice were housed in a specific pathogen-free environment. The animal experiments were performed in accordance with ARRIVE guidelines and the experimental protocol was approved by the Ethics Committee of Lanzhou University Second Hospital (approval no. D2021-136). MKN45 cells with YWHAG knockdown and MKN45 cells were injected subcutaneously into the left side of the BALB/c nude mice (n = 5 per group). NCI-N87 and NCI-N87 cells overexpressing YWHAG were also injected subcutaneously into the left side of the mice. After one week, tumor volumes (length×width^2/2) were measured at 3-day intervals. Then, on day 35, all the mice were sacrificed under deep anesthesia, and the tumors were excised for analysis.

Statistical analysis

All data were analyzed using GraphPad Prism8 software ((GraphPad Software Inc., San Diego, CA, USA). One-way analysis of variance (ANOVA) was used to analyze differences between multiple groups, and Student's *t*-test was used to analyze differences between two groups. The chi-squared test was used to analyze the correlation between YWHAG expression and clinicopathological characteristics. $p < 0.05$ was considered statistically significant.

Results

YWHAG was overexpressed in GC tissues

To identify YWHAG expression in GC tissues, we subjected 107 pairs of GC and normal adjacent tissue samples to IHC. As shown in Fig. 1A, YWHAG was mainly localized in the cytoplasm of human GC cells and was significantly upregulated in GC tissues compared to normal tissues ($p < 0.0001$; Fig. 1B). Further, based on TCGA database, YWHAG expression was higher in GC tissue than in normal tissue ($p < 0.0001$) (Fig. 1C). Furthermore, median YWHAG IHC scores showed that patients with GC could be divided into the low and high YWHAG expression groups, and as shown in Table 1, increased YWHAG expression was significantly correlated with a poor degree of differentiation. However, YWHAG expression did not show any significant correlation with other clinicopathological features. These findings suggested the possibility of an association between YWHAG overexpression and malignant GC progression.

Table 1
Correlation between YWHAG expression and clinical characteristics.

Characteristics	Low YWHAG expression	High YWHAG expression	*P*-value
Age (years)			0.723
≤ 60	26	38	
> 60	16	27	
Gender			0.654
Male	28	46	
Female	14	19	
Lauren classification			0.288
Intestinal	22	24	
Diffuse	12	25	
Mixed	8	16	
Differentiation			
Poor	17	42	0.018
Moderate	23	23	
Well	2	0	
Invasion depth			0.536
T1	7	11	
T2	8	8	
T3	6	16	
T4	21	30	
Lymph node metastasis			0.847
N0	14	18	
N1	12	21	
N2	9	12	
N3	7	14	

Increased YWHAG expression promoted GC cell proliferation

YWHAG expression was detected in the six GC cell lines. Relative to GES-1 cells, MKN45 cells showed higher YWHAG expression, while NCI-N87 cells showed lower YWHAG expression (Fig. 1D). Further, the silencing and upregulation of YWHAG in MKN45 and NCI-N87 cells, respectively, using a lentiviral vector showed that Sh-YWHGA-1 and sh-YWHGA-2 significantly downregulated YWHAG expression in MKN45 cells (Fig. 1E). The efficacy of YWHAG overexpression in NCI-N87 cells is shown in Fig. 1F. Additionally, as shown in Fig. 2A, cell proliferation was markedly inhibited after YWHAG knockdown, whereas YWHAG overexpression promoted GC cell proliferation (Fig. 2A). EdU assay results were consistent with the CCK8 results, indicating that YWHAG notably promoted GC cell proliferation (Fig. 2B, C).

YWHAG knockdown promoted apoptosis and induced cell cycle arrest of GC cells

YWHAG knockdown induced apoptosis in GC cells. Notably, the sh-NC group was more susceptible to apoptosis under YWHAG knockdown (Fig. 2D), whereas YWHAG overexpression inhibited apoptosis in NCI-N87 cells (Fig. 2E). To determine whether YWHAG influenced GC cell cycle, flow cytometry was performed. As shown in Fig. 2F, YWHAG knockdown resulted in strong cell cycle arrest at the G0/G1 phase. In contrast, the number of cells overexpressing YWHAG in the G1 phase decreased significantly.

YWHAG enhanced cell migration and invasion in GC

Wound-healing assay was performed to investigate cell migration showed that YWHAG knockdown inhibited the migration of MKN45 cells, while an opposite observation was made for the YWHAG overexpression group (Fig. 3A, B). Furthermore, transwell assay results indicated that YWHAG overexpression also enhanced GC cell invasion (Fig. 3C, D).

YWHAG knockdown inhibited GC cells tumorigenesis in vivo

To investigate how YWHAG regulates GC progression in vivo, we constructed a subcutaneous tumor-forming nude mouse model and investigated the effects of YWHAG expression in vivo. Our results showed a significantly lower tumor growth rate and tumor volume for the YWHAG knockdown group than for the control group (Fig. 3E). In contrast, tumor growth was significantly accelerated in the YWHAG overexpression group (Fig. 3F). Additionally, we observed a decrease in Ki67 expression in the YWHAG knockdown group (Fig. 3G). Therefore, YWHAG accelerated GC tumor growth in vivo.

YWHAG activated the PI3K/AKT pathway to facilitate cell cycle arrest and EMT

GSEA performed to explore the roles of YWHAG in regulating GC progression demonstrated the enrichment of YWHAG expression in cell cycle, pyrimidine metabolism, and p53 signaling pathways (Fig. 4A, B). To clarify the mechanism by which YWHAG contributed to GC progression, we further examined cell cycle regulators. Thus, we observed decreased Cyclin D1 and CDK2 levels in the YWHAG knockdown group, while their levels in the YWHAG overexpression group increased (Fig. 5A, B). These findings suggested that YWHAG effectively inhibited the expression of CDK2 and cyclin D1 to arrest the

cell cycle in the G0/G1 phase. EMT is involved in cell invasion and metastasis[11]. Thus, we speculated that YWHAG might affect EMT in GC. As shown in Fig. 5C, YWHAG knockdown enhanced E-cadherin expression and decreased the expression of the mesenchymal phenotype-related protein, vimentin. Conversely, YWHAG overexpression promoted EMT (Fig. 5D). These findings suggested that YWHAG may regulate the cell cycle and EMT processes in GC cells, which are related to the characteristics of cancer metastasis. We further performed western blotting to evaluate whether YWHAG affected the cell cycle and EMT via the PI3K/AKT pathway. The results revealed that in the YWHAG knockdown group, the phosphorylation levels of PI3K and AKT were significantly increased, while the opposite observations were made for the YWHAG overexpression group (Fig. 5E).

Discussion

Current understanding suggests that YWHAG is involved in the progression of malignancy. Raungrut et al. showed that in lung cancer, the degree of malignancy is positively correlated with the expression level of YWHAG[12]. It has also been demonstrated that YWHAG is upregulated in various cancers and mediates oncogenic transformation [6, 7, 9]. In this study, our findings showed elevated YWHAG expression in GC tissues as well as a positive association between YWHAG expression and a high risk of poor differentiation. Additionally, YWHAG overexpression enhanced the proliferation, migration, and tumorigenicity of GC cells, whereas its knockdown exhibited the opposite effect. Further investigations also revealed that YWHAG could also play a carcinogenic role by accelerating G0/G1 cell cycle transformation and promoting EMT.

Cytokine remodeling and migration constitute the two main functions of YWHA protein. It has also been shown that YWHAG regulates the formation of actin fibers to remodel the cytoskeleton [13], which mediates cell migration and invasion [14]. Our study demonstrated that YWHAG knockdown significantly inhibited the invasion and migration of GC cells. In the tumor microenvironment, hypoxia and TGF-β stimulate the expression of specific transcription factors, namely, Snai1, Slug, Twist, and ZEB1, to initiate EMT[15]. Compared to benign tumors, higher-grade and more aggressive tumors are characterized by higher expression levels of the YWHAG/Snai1 complex [16]. Considering the critical role of YWHAG in EMT, the expression levels of EMT-related proteins were determined. The results thus obtained indicated that YWHAG knockdown inhibited EMT. However, further research is required to determine whether YWHAG affects EMT progression by forming a complex with Snai1 or otherwise. In this study, we observed that YWHAG regulated GC cell cycle primarily by affecting the G0/G1 phase of the cell cycle. Dar et al. reported that YWHAG deficiency leads to the accumulation of Set8, a substrate of the cell cycle regulator, Cdt2, which delays the progression of the G2/M phase and inhibits cell proliferation [17]. However, based on the results of this study, YWHAG did not affect the progression of the G2/M phase in GC cell cycle.

The PI3K/AKT signaling pathway, which is frequently deregulated in cancer, plays a very important role in several processes, including cell proliferation, angiogenesis, metastasis, and autophagy [18–20]. Notably, abnormal PI3K/AKT signaling can inhibit the tumorigenicity of glioma stem cells [21, 22].

Additionally, the PI3K/AKT signaling pathway mediates cisplatin resistance in GC [23, 24]. It has also been reported that miR-107 enhances the proliferation, migration, and invasion capacities of cancer cells by targeting FAT4 in the PI3K/AKT pathway [25]. AK023391 also activates PI3K/AKT to promote GC tumorigenesis [26]. Previous studies have shown that the YWHA family is important for maintaining balance in the PI3K/AKT protein network [27]. Additionally, in that in lung cancer, YWHAG activates the PI3K/AKT pathway to function as an oncogene [28], and in hematopoietic tumors, IL-3 activates the PI3K signaling pathway by inducing YWHAG overexpression, thereby regulating cell cycle progression, growth, and apoptosis [29]. Cell cycle is also regulated by the PI3K/AKT signaling pathway [30, 31]. Thus, the downstream cell cycle factors activated by the PI3K/AKT pathway facilitate cell proliferation and tumor progression. YWHAG inhibits apoptosis by interacting with TSC2, a key mediator of the PI3K pathway [28]. Studies have also revealed that angiopoietin-like 4 (AngPTL4) interacts with YWHAG via the PI3K/AKT signaling pathway and finally activates transcription factor, STAT3 to stabilize EMT-related proteins and affect EMT capacity and metastasis [16]. In this study, we performed western blot analysis to determine whether YWHAG knockdown inhibited PI3K/AKT pathway activation. Thus, we observed that YWHAG knockdown significantly reduced phosphorylated PI3K and AKT protein levels, indicating that YWHAG is involved in the PI3K/AKT signaling pathway. However, whether YWHAG activated this signaling pathway through the key downstream genes of PI3K requires further investigation. Based on our observations, we concluded that YWHAG participates in proliferation and EMT in GC and these effects may be attributed to PI3K/AKT signaling. However, whether YWHAG has an upstream target or interacts with AngPTL4 remains to be clarified. Studies in this regard will also constitute a research hotspot in future.

In conclusion, the results of study indicated that YWHAG is overexpressed in GC tissues and may stimulate cell proliferation and migration via the PI3K/AKT signaling pathway. Therefore, targeting YWHAG may be a crucial therapeutic option for precise human GC treatment.

Declarations

Acknowledgments: We would like to thank Editage (www.editage.cn) for English language editing.

Author contributions: YL, LY, YG, and JL conceived the study. LY and YG proposed the methodology for this study. LY, YG, and XL performed data validation. SW and JL visualized the results; LY and YG wrote the draft manuscript. YL and LY reviewed and edited the manuscript.

Funding: This work was supported by the National Natural Science Foundation of China (grant number 31770537) and the Cuiying Scientific and Technological Innovation Program of Lanzhou University Second Hospital (grant number CY2022-QN-A19).

Ethical approval: This study was conducted in accordance with the principles of the Declaration of Helsinki, and was approved by the Ethics Committee of Lanzhou University Second Hospital (Date 2021-3-18/Approval No. 2021A-153 and Date 2021-3-17/Approval No. D2021-136).

Conflicts of interest: The authors declare no conflicts of interest.

Data Availability Statement

The data generated or analyzed during this study can be available from the corresponding author on reasonable request.

References

1. Smyth EC, Nilsson M, Grabsch HI, van Grieken NCT, Lordick F: Gastric cancer. The Lancet 2020, 396(10251):635–648.
2. Global Burden of Disease Cancer C, Fitzmaurice C, Akinyemiju TF, Al Lami FH, Alam T, Alizadeh-Navaei R, Allen C, Alsharif U, Alvis-Guzman N, Amini E *et al*: Global, Regional, and National Cancer Incidence, Mortality, Years of Life Lost, Years Lived With Disability, and Disability-Adjusted Life-Years for 29 Cancer Groups, 1990 to 2016: A Systematic Analysis for the Global Burden of Disease Study. JAMA Oncol 2018, 4(11):1553–1568.
3. Li Y, Xu C, Wang B, Xu F, Ma F, Qu Y, Jiang D, Li K, Feng J, Tian S *et al*: Proteomic characterization of gastric cancer response to chemotherapy and targeted therapy reveals new therapeutic strategies. Nature communications 2022, 13(1):5723.
4. Fan X, Cui L, Zeng Y, Song W, Gaur U, Yang M: 14-3-3 Proteins Are on the Crossroads of Cancer, Aging, and Age-Related Neurodegenerative Disease. International journal of molecular sciences 2019, 20(14).
5. Horie M, Suzuki M, Takahashi E, Tanigami A: Cloning, expression, and chromosomal mapping of the human 14-3-3gamma gene (YWHAG) to 7q11.23. Genomics 1999, 60(2):241–243.
6. Wang H, Zhi H, Ma D, Li T: MiR-217 promoted the proliferation and invasion of glioblastoma by repressing YWHAG. Cytokine 2017, 92:93–102.
7. Wang P, Deng Y, Fu X: MiR-509-5p suppresses the proliferation, migration, and invasion of non-small cell lung cancer by targeting YWHAG. Biochemical and biophysical research communications 2017, 482(4):935–941.
8. Hiraoka E, Mimae T, Ito M, Kadoya T, Miyata Y, Ito A, Okada M: Breast cancer cell motility is promoted by 14-3-3gamma. Breast Cancer 2019, 26(5):581–593.
9. Yoo JO, Kwak SY, An HJ, Bae IH, Park MJ, Han YH: miR-181b-3p promotes epithelial-mesenchymal transition in breast cancer cells through Snail stabilization by directly targeting YWHAG. Biochimica et biophysica acta 2016, 1863(7 Pt A):1601–1611.
10. Mei J, Liu Y, Xu R, Hao L, Qin A, Chu C, Zhu Y, Liu X: Characterization of the expression and prognostic value of 14-3-3 isoforms in breast cancer. Aging 2020, 12(19):19597–19617.
11. Dongre A, Weinberg RA: New insights into the mechanisms of epithelial-mesenchymal transition and implications for cancer. Nat Rev Mol Cell Biol 2019, 20(2):69–84.

12. Raungrut P, Wongkotsila A, Champoochana N, Lirdprapamongkol K, Svasti J, Thongsuksai P: Knockdown of 14-3-3gamma Suppresses Epithelial-Mesenchymal Transition and Reduces Metastatic Potential of Human Non-small Cell Lung Cancer Cells. Anticancer Res 2018, 38(6):3507–3514.
13. Abdrabou A, Brandwein D, Liu C, Wang Z: Rac1 S71 Mediates the Interaction between Rac1 and 14-3-3 Proteins. Cells 2019, 8(9).
14. Fife CM, McCarroll JA, Kavallaris M: Movers and shakers: cell cytoskeleton in cancer metastasis. Br J Pharmacol 2014, 171(24):5507–5523.
15. Georgakopoulos-Soares I, Chartoumpekis DV, Kyriazopoulou V, Zaravinos A: EMT Factors and Metabolic Pathways in Cancer. Frontiers in oncology 2020, 10:499.
16. Teo Z, Sng MK, Chan JSK, Lim MMK, Li Y, Li L, Phua T, Lee JYH, Tan ZW, Zhu P *et al*: Elevation of adenylate energy charge by angiopoietin-like 4 enhances epithelial-mesenchymal transition by inducing 14-3-3gamma expression. Oncogene 2017, 36(46):6408–6419.
17. Dar A, Wu D, Lee N, Shibata E, Dutta A: 14-3-3 proteins play a role in the cell cycle by shielding cdt2 from ubiquitin-mediated degradation. Molecular and cellular biology 2014, 34(21):4049–4061.
18. Alzahrani AS: PI3K/Akt/mTOR inhibitors in cancer: At the bench and bedside. Seminars in cancer biology 2019, 59:125–132.
19. Aoki M, Fujishita T: Oncogenic Roles of the PI3K/AKT/mTOR Axis. Current topics in microbiology and immunology 2017, 407:153–189.
20. Xu Z, Han X, Ou D, Liu T, Li Z, Jiang G, Liu J, Zhang J: Targeting PI3K/AKT/mTOR-mediated autophagy for tumor therapy. Applied microbiology and biotechnology 2020, 104(2):575–587.
21. Chai C, Song LJ, Han SY, Li XQ, Li M: MicroRNA-21 promotes glioma cell proliferation and inhibits senescence and apoptosis by targeting SPRY1 via the PTEN/PI3K/AKT signaling pathway. CNS neuroscience & therapeutics 2018, 24(5):369–380.
22. Ma L, Gai J, Qiao P, Li Y, Li X, Zhu M, Li G, Wan Y: A novel bispecific nanobody with PD-L1/TIGIT dual immune checkpoint blockade. Biochemical and biophysical research communications 2020, 531(2):144–151.
23. Dai Q, Zhang T, Pan J, Li C: LncRNA UCA1 promotes cisplatin resistance in gastric cancer via recruiting EZH2 and activating PI3K/AKT pathway. Journal of Cancer 2020, 11(13):3882–3892.
24. Zheng P, Chen L, Yuan X, Luo Q, Liu Y, Xie G, Ma Y, Shen L: Exosomal transfer of tumor-associated macrophage-derived miR-21 confers cisplatin resistance in gastric cancer cells. Journal of experimental & clinical cancer research: CR 2017, 36(1):53.
25. Wei R, Xiao Y, Song Y, Yuan H, Luo J, Xu W: FAT4 regulates the EMT and autophagy in colorectal cancer cells in part via the PI3K-AKT signaling axis. Journal of experimental & clinical cancer research: CR 2019, 38(1):112.
26. Huang Y, Zhang J, Hou L, Wang G, Liu H, Zhang R, Chen X, Zhu J: LncRNA AK023391 promotes tumorigenesis and invasion of gastric cancer through activation of the PI3K/Akt signaling pathway. Journal of experimental & clinical cancer research: CR 2017, 36(1):194.

27. Rietscher K, Keil R, Jordan A, Hatzfeld M: 14-3-3 proteins regulate desmosomal adhesion via plakophilins. Journal of cell science 2018, 131(10).
28. Radhakrishnan VM, Martinez JD: 14-3-3gamma induces oncogenic transformation by stimulating MAP kinase and PI3K signaling. PLoS One 2010, 5(7):e11433.
29. Ajjappala BS, Kim YS, Kim MS, Lee MY, Lee KY, Ki HY, Cha DH, Baek KH: 14-3-3 gamma is stimulated by IL-3 and promotes cell proliferation. Journal of immunology (Baltimore, Md: 1950) 2009, 182(2):1050–1060.
30. Lee HJ, Venkatarame Gowda Saralamma V, Kim SM, Ha SE, Raha S, Lee WS, Kim EH, Lee SJ, Heo JD, Kim GS: Pectolinarigenin Induced Cell Cycle Arrest, Autophagy, and Apoptosis in Gastric Cancer Cell via PI3K/AKT/mTOR Signaling Pathway. *Nutrients* 2018, 10(8).
31. Liu JS, Huo CY, Cao HH, Fan CL, Hu JY, Deng LJ, Lu ZB, Yang HY, Yu LZ, Mo ZX *et al*: Aloperine induces apoptosis and G2/M cell cycle arrest in hepatocellular carcinoma cells through the PI3K/Akt signaling pathway. Phytomedicine: international journal of phytotherapy and phytopharmacology 2019, 61:152843.

Figures

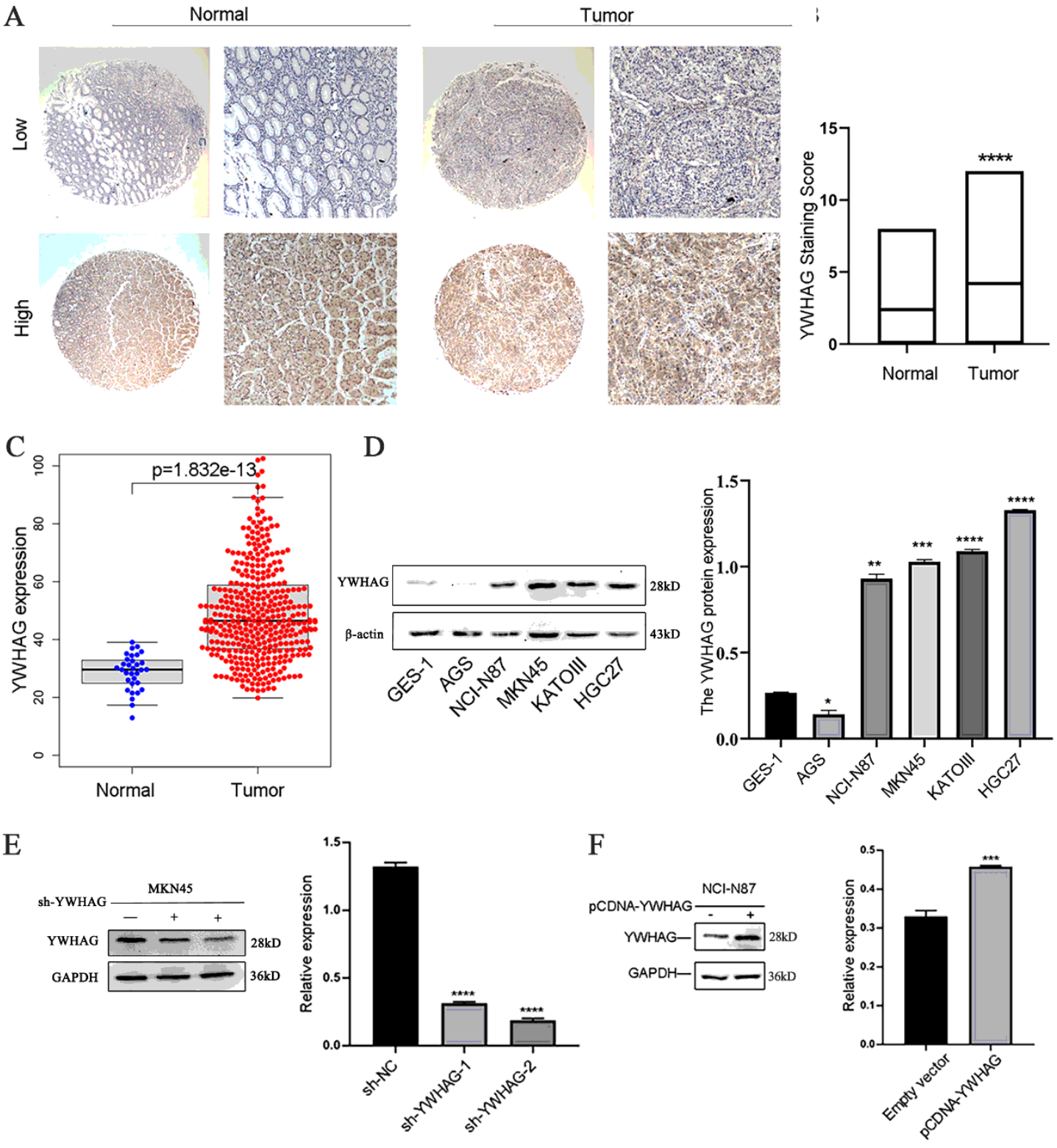

Figure 1

YWHAG expression. (A) Representative images for YWHAG expression in gastric cancer (GC) and normal tissues. (B) YWHAG upregulation in GC tissues. (C) YWHAG mRNA expression of GC tissue samples in TCGA database. (D) YWHAG expression in GC cells determined via western blot analysis. (E, F) YWHAG knockdown and overexpression efficiencies verified via western blot analysis.

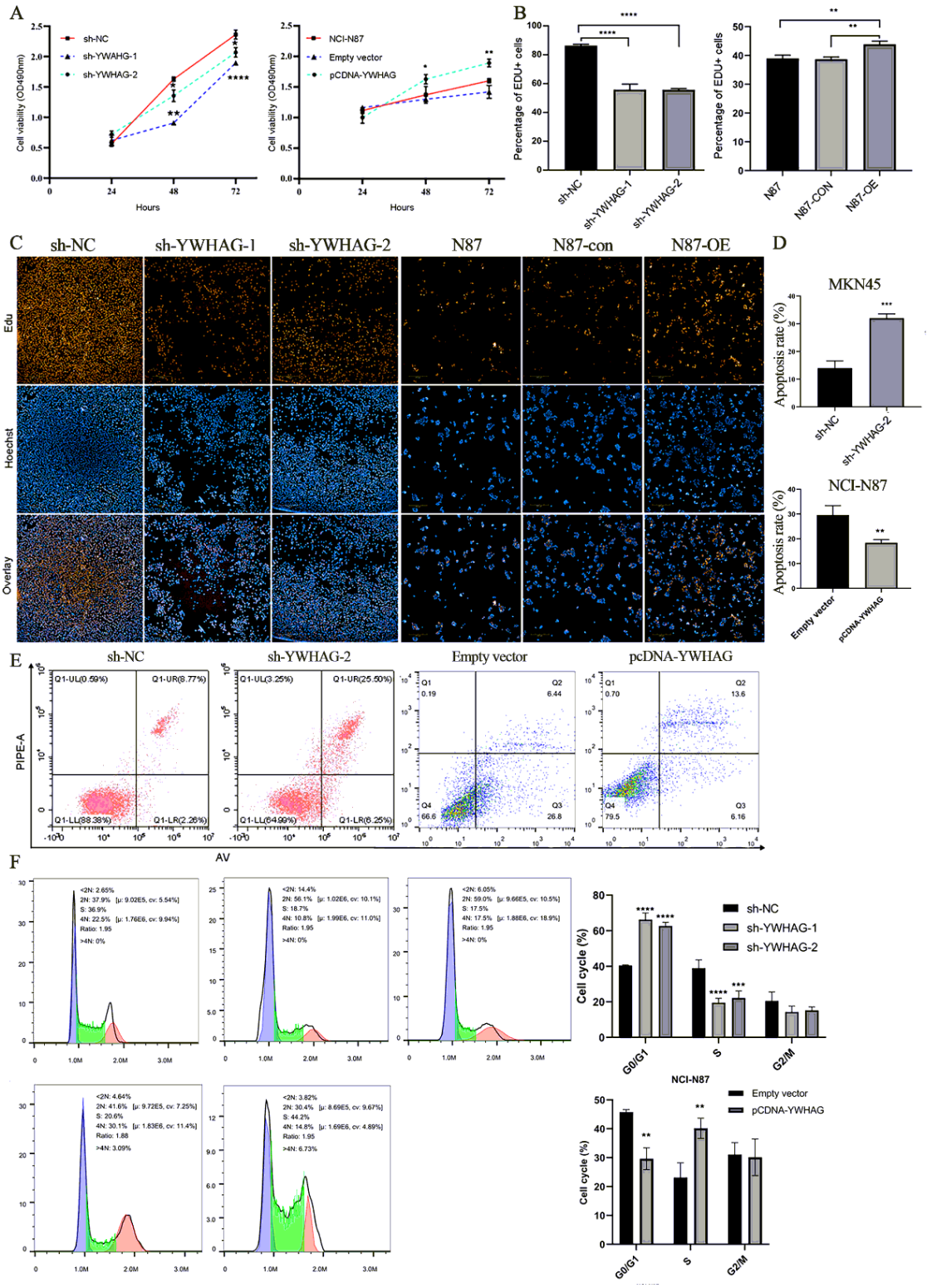

Figure 2

YWHAG promoted the proliferation of GC cells. (A) CCK8 assays showing the proliferation of MKN45 and NCI-N87 cells. (B) Data from EdU assays. (C) EdU assays of YWHAG knockdown and overexpression cells. (D) Data for apoptosis. (E) YWHAG knockdown induced apoptosis in MKN45 cells and YWHAG overexpression inhibited apoptosis. (F) Cell cycle analysis of MKN45 and NCI-N87 cells.

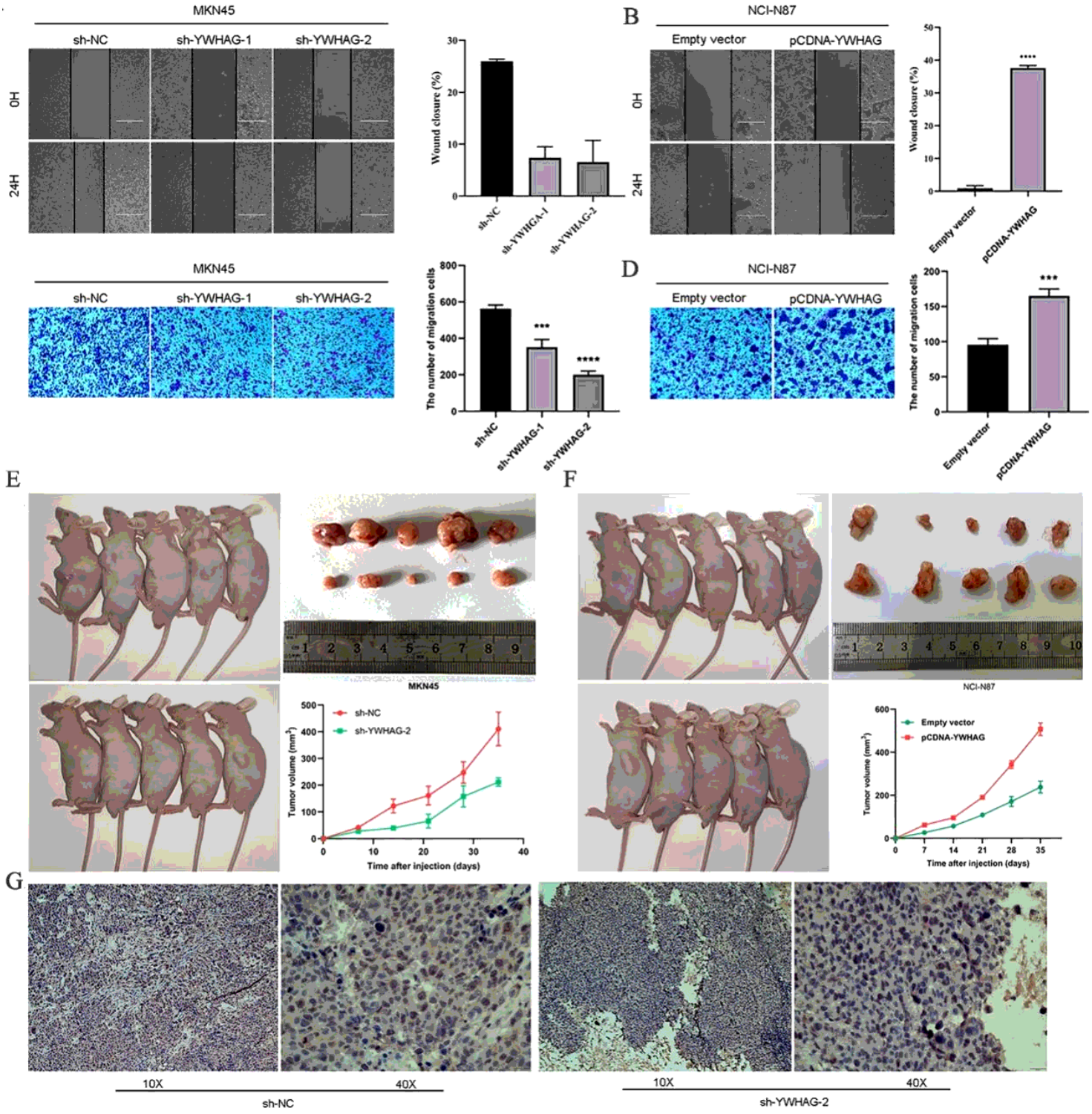

Figure 3

YWHAG promoted GC cell invasion. (A, B) Wound-healing assay in MKN45 and NCI-N87 cells. (C, D) Transwell assay of MKN45 and NCI-N87 cells. (E) Smaller tumor sizes owing to YWHAG knockdown cells compared to sh-NC cells. (F) Larger tumors owing to YWHAG overexpression cells compared with the control group. (G) Ki67 expression in MKN45 xenograft tumors.

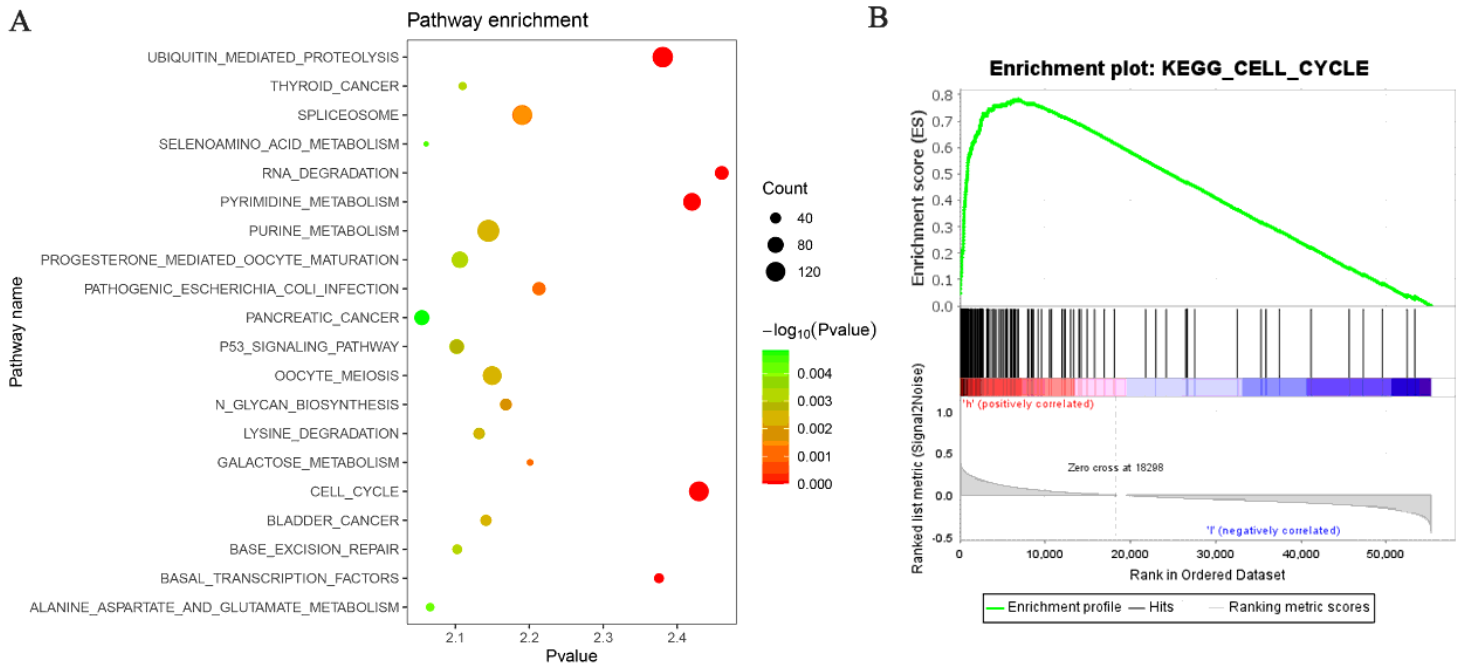

Figure 4

GSEA analysis of YWHAG in GC cells. (A) GSEA of YWHAG in GC. (B) YWHAG enriched in the cell cycle.

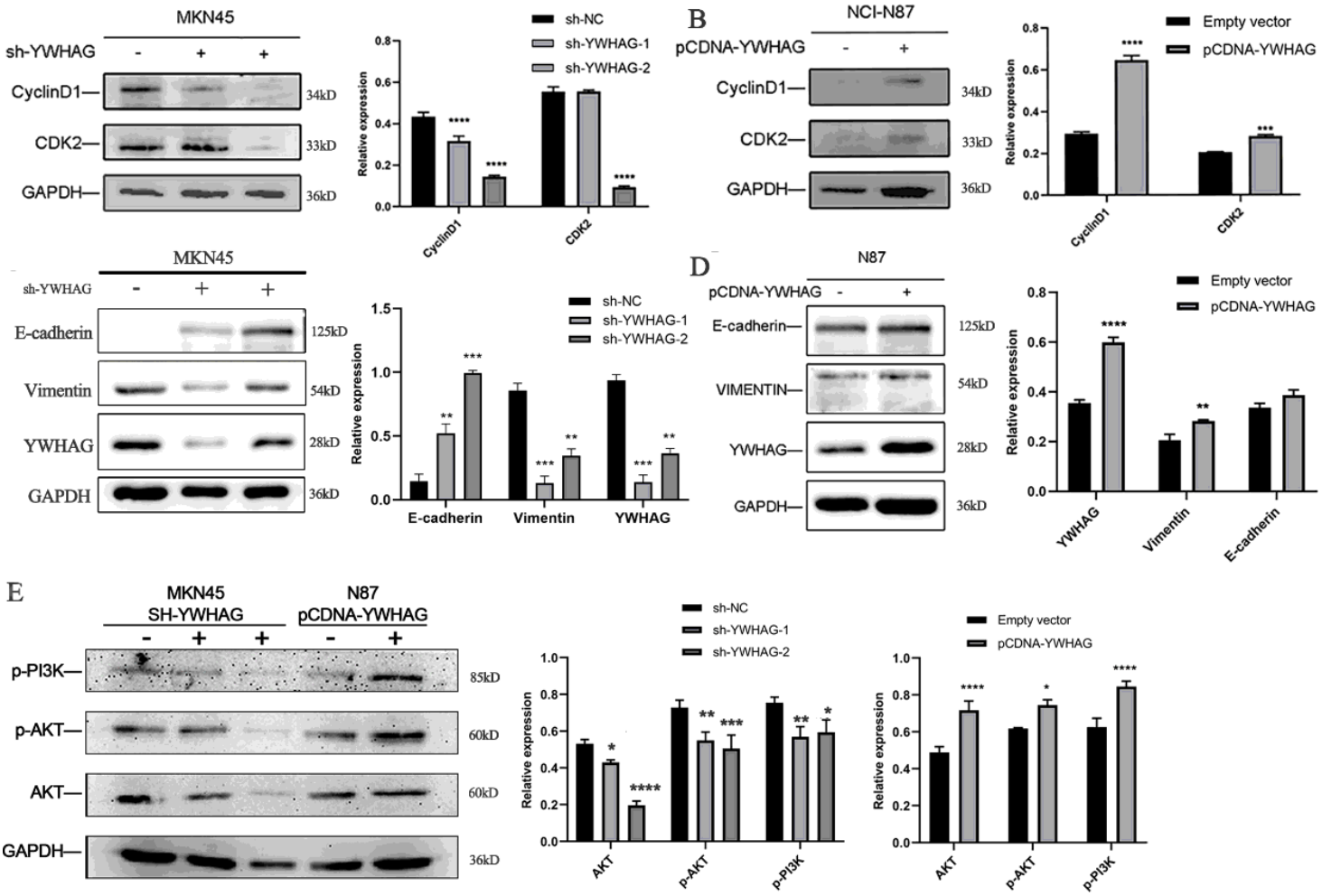

Figure 5

Mechanisms of the action of YWHAG in GC cells. (A, B) Expression of cell-cycle regulators in MKN45 and NCI-N87 cells. (C, D) Expression of E-cadherin and vimentin in MKN45 and NCI-N87 cells determined via western blot analysis. (E) Expression of AKT, p-PI3K, and p-AKT in MKN45 and NCI-N87 cells determined via western blot analysis.

Supplementary Files

This is a list of supplementary files associated with this preprint. Click to download.

- 1E.zip
- 1D.zip
- 1F.zip
- 5E.zip
- 5A.zip
- 5D.zip
- 5B.zip
- 5C.zip